

Electrochemical Promotion of a Dispersed Platinum Catalyst

M. Marwood and C. G. Vayenas

Department of Chemical Engineering, University of Patras, Patras GR-26500, Greece

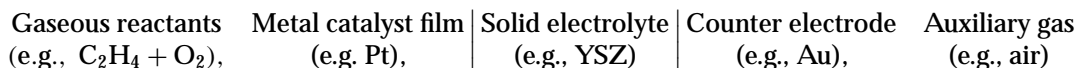
Received July 15, 1997; revised March 2, 1998; accepted May 12, 1998

The effect of electrochemical promotion or nonfaradaic electrochemical modification of catalytic activity (NEMCA effect) was investigated for the first time on highly dispersed Pt catalyst (dispersion 0.2–1) supported on polycrystalline Au films which had been deposited on Y₂O₃-stabilized ZrO₂ (YSZ), an O²⁻ conductor. The oxidation of ethylene to CO₂ was chosen as a model reaction. It was found that the catalytic rate of ethylene oxidation could be reversibly enhanced by up to a factor of 5 via electrical current or potential application between the supported Pt/Au catalyst and a counter Au electrode also deposited on the YSZ ionic conductor. The increase in catalytic rate is typically a factor of 10³ higher than the rate, $I/2F$, of electrochemical supply or removal of O²⁻ to (from) the dispersed Pt/Au catalyst from (to) the solid electrolyte. Analysis of the time constant of the catalytic rate upon current application or interruption suggests that, as in previous electrochemical promotion studies with continuous metal film catalysts, the observed promotional phenomena are due to electrochemically controlled migration (spillover and backspillover) of anionic oxygen between the solid electrolyte and the metal catalyst surface and to the effect of this anionic oxygen on the chemisorptive bond strength of coadsorbed oxygen and ethylene. © 1998 Academic Press

INTRODUCTION

The effect of electrochemical promotion or nonfaradaic electrochemical modification of catalytic activity (NEMCA effect) (1–12) has been studied for over 40 catalytic reactions on Pt, Pd, Rh, Fe, Ni, and Ag catalyst films deposited on several types of solid electrolytes, including O²⁻ conductors (e.g., Y₂O₃-stabilized ZrO₂, YSZ), Na⁺ conductors (e.g., Na-β''-Al₂O₃ and Nasion), F⁻ conductors (e.g., CaF₂), H⁺ conductors (Nafion (7), Ca_{0.9}ZrIn_{0.1}O_{3-α} (8)) and mixed conductors (e.g., TiO₂ (9), CeO₂ (10)). Work in this area has been reviewed recently (11, 12).

In brief it was found that the catalytic activity and selectivity of metal films deposited on solid electrolytes can be altered *in situ* in a very pronounced and reversible manner by applying currents or potentials (typically ±2 V) between the catalyst film and a counter electrode in galvanic cells of the type:



In the so-called “single pellet” design (11, 12), both the catalyst and the counter electrode are exposed to the reacting gas mixture and, thus, the auxiliary gas is the reacting gas mixture itself.

The main parameters used to describe the magnitude of electrochemical promotion for different catalytic systems are:

- The enhancement factor, or faradaic efficiency, Λ , defined from

$$\Lambda = \Delta r / (I/2F), \quad [1]$$

where Δr is the electrochemically induced change in catalytic rate r ; I is the applied current (defined positive when anions are supplied to the catalyst); and F is Faraday's constant. A reaction exhibits electrochemical promotion when $|\Lambda| > 1$. When $\Lambda > 1$ the catalytic reaction is termed electrophobic and when $\Lambda < -1$ the reaction is termed electrophilic (11, 12).

- The rate enhancement ratio, ρ , defined from

$$\rho = r / r^o, \quad [2]$$

where r^o is the open-circuit, unpromoted catalytic rate.

The origin of electrochemical promotion has been studied using catalytic rate transient analysis (11, 12), cyclic voltammetry (13), work function measurements (2, 12), X-ray photoelectron spectroscopy (XPS) (14, 15), temperature-programmed desorption (TPD) (16), scanning tunneling microscopy (STM) (17), and *ab initio* quantum mechanical calculations (18). All these investigations have provided strong evidence that electrochemical promotion is due to the catalytically promoting action of ionic species which migrate (backspillover) onto the catalyst film surface under the influence of the applied potential.

Both TPD (16) and quantum mechanical calculations (18) have shown clearly that the chemisorptive bond strength of coadsorbed catalytically active species varies significantly upon varying the catalyst potential and work function (2) and thus the coverage of promoting ionic

species (14, 15, 17). This can then explain the observed pronounced modification of the catalytic rates (11, 12).

Previous electrochemical promotion studies were limited to massive continuous (albeit porous) metal films with a grain size typically of the order of a micrometer (11, 12), thus rather low surface area (typically $5\text{--}500\text{ cm}^2/\text{cm}^2$ of solid electrolyte), and thus very low metal dispersion (typically less than 10^{-4} (11, 12)).

From a practical viewpoint, in order to compete favourably with classical supported catalysts, an electrochemically promoted catalyst should ideally have comparable metal dispersion, i.e. typically above 0.1 (19). The present work is the first effort in this direction when using solid electrolytes. It should be noted, however, that highly dispersed Pt/graphite catalysts have already been used for electrochemical promotion studies of H_2 oxidation in aqueous alkaline solutions (20).

In the present study a highly dispersed Pt catalyst (Pt dispersion $D \approx 0.2$ or higher) was deposited on a porous Au film which was practically inactive for C_2H_4 oxidation and was supported on an YSZ-solid electrolyte. Detailed kinetic and electrochemical promotion experiments were performed at temperatures below 450°C , where Pt-Au alloy formation, which is endothermic, does not take place (21). It was found that the dispersed Pt catalyst can be electrochemically promoted, apparently due to electrochemically controlled oxide ion backspillover over the Au electrode surface to the dispersed Pt crystallites. These results have shown that, in principle, it is possible to utilize electrochemical promotion with highly dispersed catalysts which are not necessarily in contact with the solid electrolyte but are dispersed on an electronically conducting material interfaced with the solid electrolyte. This may turn out to be of significant practical importance although, of course, electrically conducting support materials other than Au must be examined for future potential practical applications.

EXPERIMENTAL

The apparatus utilizing gas chromatography and an IR CO_2 analyzer for reactants and products analysis has been described previously (1, 9, 11, 12). The atmospheric pressure well-mixed (11) single-pellet quartz reactor is shown in Fig. 1, together with the catalyst and electrode configuration. Reactants were Messer-Griesheim certified standard mixtures of 4% C_2H_4 in He and synthetic air. They could be further diluted in ultrapure (99.999%) He.

Gold reference and counter electrodes were deposited on one side of a YSZ disk (Didier Werke AG; 19-mm diameter, 3-mm thickness) while a gold working electrode, totally covering the exposed YSZ surface, was deposited on the other side of the disk. These porous gold films were obtained by using a Au paste prepared by mixing Aldrich Au powder (99.9%+) in a slurry of polyvinyl acetate binder

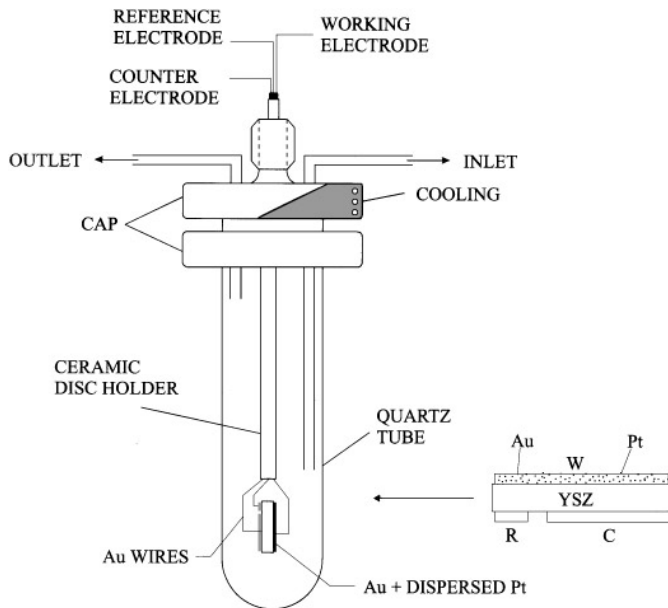


FIG. 1. Single pellet catalytic reactor and electrode configuration.

in ethyl acetate, calcined in air first for 2 h at 400°C and then at 900°C for another 2 h.

The catalytic and electrocatalytic activity of the gold working electrode was measured at that stage. A small catalytic rate of $r = 2 \times 10^{-8}$ mol O/s was measured for ethylene oxidation at 425°C and a gaseous composition of $P_{\text{C}_2\text{H}_4} = 0.7\text{ kPa}$ and $P_{\text{O}_2} = 17.1\text{ kPa}$. This small activity can be attributed to trace impurities in the gold films and is more apparent in this system as compared to former NEMCA studies due to the larger quantities of gold employed for the working electrode. However, no modification of this rate was observed when a negative or positive potential was applied. Consequently all the observed potential-induced rate modifications can be safely attributed to the dispersed Pt catalyst only. In the present communication, as in previous NEMCA studies of catalytic oxidations (11, 12) the catalytic rate is expressed in mol O/s.

Platinum was subsequently dispersed on the gold working electrode following a wet impregnation procedure. A small tubular compartment was formed by sealing the YSZ pellet at one end of a polymer tube of appropriate diameter, with the working electrode in the interior of this compartment. Subsequently 1.8 ml of a 10^{-8} mol/ml solution of H_2PtCl_6 in water were introduced in this container and heated to 80°C and 90°C for catalyst samples C_1 and C_2 , respectively, until the water of the solution had been evaporated. The pellet was then calcined in air at 450°C for 1h, mounted in the single pellet reactor (Fig. 1) and reduced *in situ* for 2 h in a flow of 60 ml/min of 2% H_2 in He at a temperature of 250°C .

The resulting dispersion of the Pt was measured at the end of the kinetic experiments for sample C_2 by surface

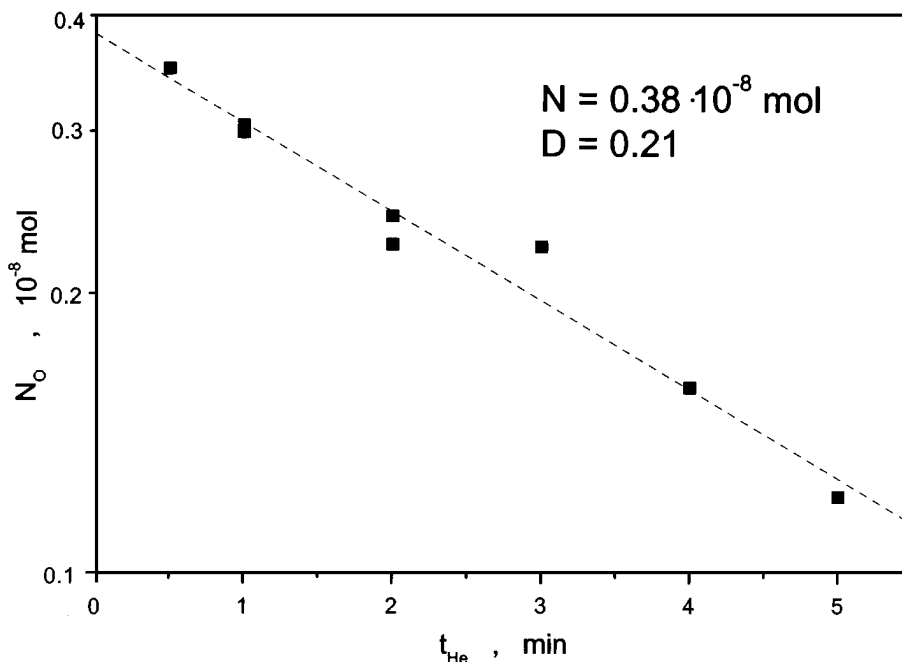


FIG. 2. Effect of desorption time t_{He} on the amount, N_{O} , of oxygen consumed (expressed in mol O) by the reaction of O_2 with adsorbed carbon monoxide. The maximum amount, N , of CO adsorbed is obtained by extrapolating to $t_{\text{He}} = 0$. Conditions: catalyst C2, $T = 256^\circ\text{C}$, adsorption = 500 ml/min of 1% CO; purge = 340 ml/min of He; titration = 47.2 ml/min of 21% O_2 .

titration of CO by oxygen, following the technique described by Stoukides and Vayenas (22). In brief, carbon monoxide was adsorbed on the Pt surface at 256°C while a flow a 500 ml/min of 1% CO in He was passed through the reactor. The gas phase in the reactor was then purged using a flow of 340 ml/min of He at the same temperature during a purging time, t_{He} , at least eight times longer than the residence time of the reactor. A flow of 47 ml/min of 21% O_2 was then passed through the reactor and the amount of CO_2 formed, or oxygen consumed, N_{O} , was measured by integrating the resulting CO_2 peak measured by a CO_2 IR-analyser. This procedure was repeated for different purging times t_{He} , ranging from 30 s to 5 min, and the maximum reactive CO uptake, N , was obtained by extrapolating to $t_{\text{He}} = 0$. A value of $N = 0.38 \times 10^{-8}$ mol is thus obtained (Fig. 2) for catalyst C₂. This corresponds to a dispersion of Pt of $D = 0.21$, assuming an adsorption stoichiometry of 1 : 1 for carbon monoxide on Pt. Catalyst C₁ had the same Pt mass with catalyst C₂ (1.8×10^{-8} mol) and its surface area was a factor 5 higher than that of C₁, as estimated by measuring the rate of C_2H_4 oxidation under similar operating conditions. This corresponds to almost complete Pt dispersion ($D \approx 1$).

Constant currents between the catalyst and counter electrodes, or constant potentials between the catalyst and reference electrodes were applied via an AMEL 550 galvanostat-potentiostat.

It is worth noting that when using the "single-pellet" design (11, 12, 23) the O_2 , Au/YSZ reference electrode acts

in reality as a pseudoreference since P_{O_2} is not fixed but is varied upon varying the gaseous composition during the kinetic experiments. Furthermore, the surface oxygen activity, a_{O}^2 (11, 12), may in general be lower than P_{O_2} if a fast catalytic reaction, e.g. C_2H_4 oxidation, takes place on the Au surface. The choice of Au is thus dictated by its low catalytic activity for C_2H_4 oxidation. Previous electrochemical promotion studies of C_2H_4 oxidation (23, 24) have shown that Au acts as a good pseudoreference electrode since its potential varies little with gaseous composition, typically less than 0.1 V, over the gas composition range of the present investigation. It may thus be considered (within $0.1 \pm V$) as an oxygen reference electrode. At $P_{\text{O}_2} = 0.21$ atm, V_{WR} is near 0 V and the corresponding work function value of Au is 5 (+0.1) eV (11, 25). Since the work function scale can be directly related to the aqueous electrochemistry NHE scale (26) this information could, in principle, be useful for the future establishment of a correspondence between the aqueous electrochemistry NHE scale and the high temperature electrochemistry scale, where, as in the present work, the O_2 , Au/YSZ, or, equivalently, O_2 , Pt/YSZ electrode is frequently used (11, 12).

RESULTS

Galvanostatic Catalytic Transients

Figure 3 shows the transient effect of a negative current application and interruption on the rate of C_2H_4 oxidation.

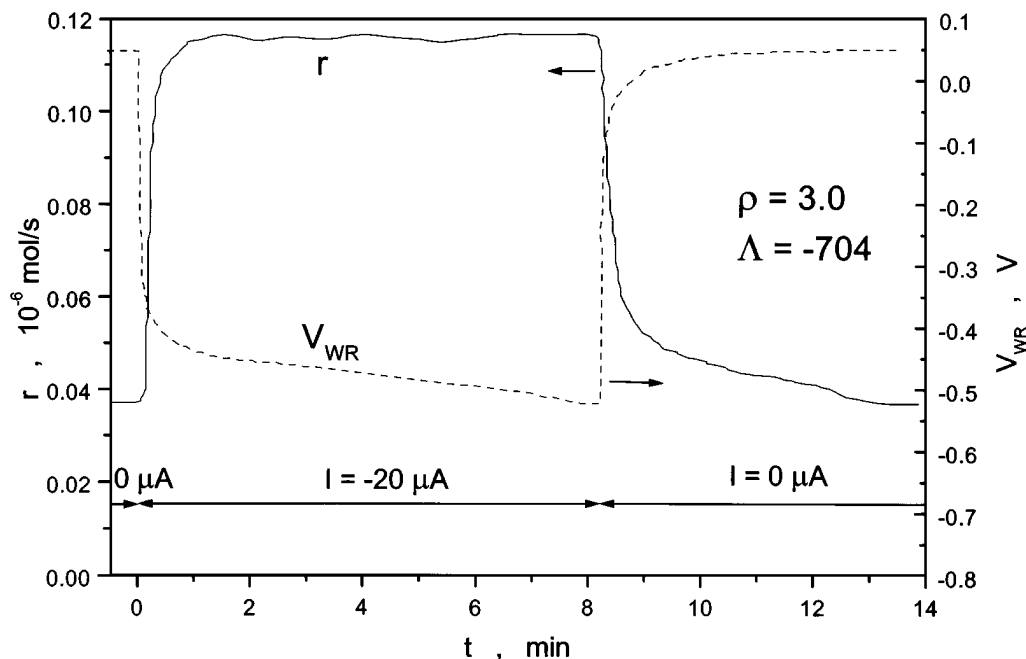


FIG. 3. Transient effect of an applied negative current ($I = -20$ mA) on the reaction rate r (solid curve) and on the catalyst potential V_{WR} (dashed curve). Conditions: catalyst C2, $T = 421^\circ\text{C}$, $P_{O_2} = 14.8$ kPa, $P_{C_2H_4} = 0.1$ kPa, flow = 411 ml/min, open circuit rate: $r_0 = 0.037 \times 10^{-6}$ mol/s.

Initially ($t < 0$) the electrical circuit is open and the open-circuit (unpromoted) catalytic rate is $0.037 \mu\text{mol/s}$. The corresponding turnover frequency (TOF, i.e. oxygen atoms reacting per surface Pt atom per s) is 10 s^{-1} . At $t = 0$ a negative current ($I = -20 \mu\text{A}$) is applied between the Pt/Au catalyst and the Au counter electrode and thus O^{2-} are removed from the Pt/Au catalyst at a rate $I/2F = 1.04 \times 10^{-10}$ mol/s. This causes a threefold enhancement in the catalytic rate ($\rho = 3$). The rate increase, Δr , is 704 times larger than the rate of O^{2-} removal ($\Lambda = -704$). The negative Λ sign indicates electrophilic behaviour (11, 12); i.e., the catalytic rate is enhanced with negative current or, equivalently, decreasing catalyst potential, V_{WR} , with respect to the reference Au electrode. (The subscript "WR" denotes the potential of the working "W" electrode, i.e. the Pt/Au catalyst, with respect to the Au reference "R" electrode). It is worth noting that V_{WR} is related to the average (24) work function, $e\Phi$, of the gas-exposed catalyst surface via

$$e\Delta V_{WR} = \Delta(e\Phi) \quad [3]$$

as shown both via the Kelvin probe technique (2, 27) and via UPS measurements (28).

Upon current interruption (Fig. 3) both the catalytic rate and the catalyst potential V_{WR} return to their open-circuit value; i.e., the effect is reversible. The catalytic rate time constant, τ , during both current application and interruption is of the order of 1 min. As discussed below τ is of the same order of magnitude as $2FN/I$, where N is the Pt catalyst surface area, expressed in mol Pt and I is the applied

current. This strongly suggests that the dynamic behaviour of the system is governed by the removal of an anionic oxygen species from the Pt catalyst surface.

Figure 4 shows a galvanostatic transient obtained with a positive current, i.e. with electrochemical O^{2-} supply to the catalyst. In this experiment, performed with an ethylene partial pressure, $P_{C_2H_4}$ six times higher than that of Fig. 3, electrophilic behaviour is obtained again; i.e., the rate decreases with O^{2-} supply to the catalyst and thus with increasing potential. The rate decrease $\Delta r = -0.107 \mu\text{mol/s}$, which accounts for 37% of the open-circuit rate, is 1032 times larger than the rate of O^{2-} supply to the catalyst. The effect is again quite reversible; i.e., both rate and potential return to their open-circuit values upon current interruption.

Steady-State Effect of Potential

Figures 5a and 5b show the steady state effect of catalyst potential, V_{WR} , on the rate of ethylene oxidation for the two catalyst films, labeled C1 and C2, and for the same fuel-lean gaseous composition used to obtain the transient of Fig. 3.

The effect of potential on catalytic rate is qualitatively similar for both catalysts; i.e. the rate goes through a minimum near the open-circuit catalyst potential, V_{WR}^0 , which is near 0.1 V for both catalysts. Decreasing catalyst potential, and work function, below V_{WR}^0 causes an exponential increase in the rate, i.e.,

$$\ln(r/r^0) = \alpha F \Delta V_{WR} / RT, \quad [4]$$

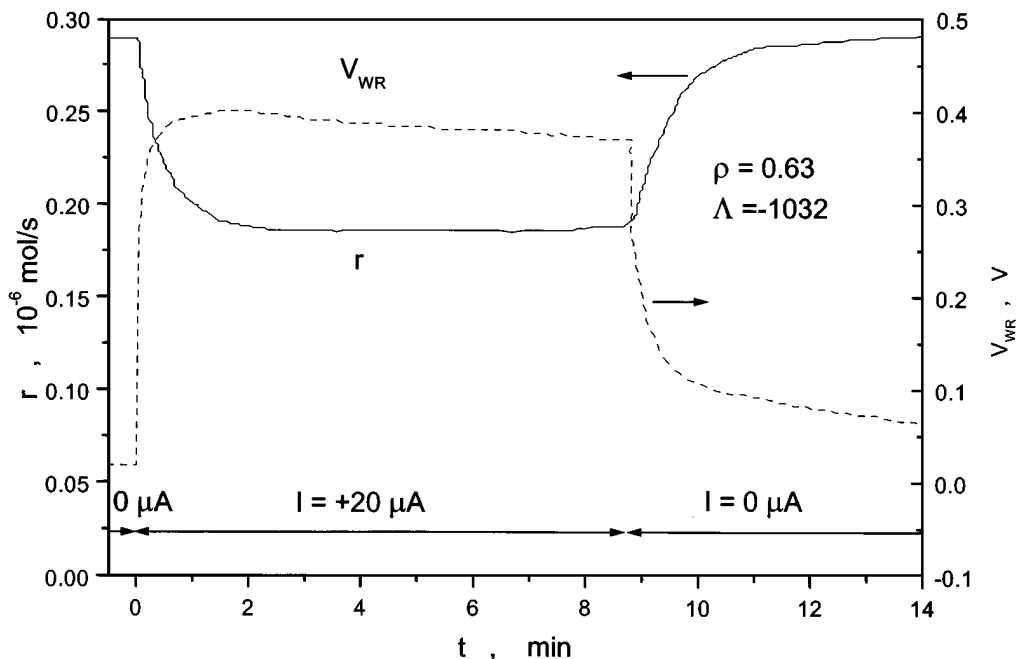


FIG. 4. Transient effect of an applied positive current ($I = +20 \mu\text{A}$) on the reaction rate r (solid curve) and on the catalyst potential V_{WR} (dashed curve). Conditions: catalyst C2, $T = 371^\circ\text{C}$, $P_{\text{O}_2} = 18.0 \text{ kPa}$, $P_{\text{C}_2\text{H}_4} = 0.6 \text{ kPa}$, flow = 206 ml/min, open-circuit rate: $r^0 = 0.293 \times 10^{-6} \text{ mol/s}$.

where the NEMCA parameter α (11, 12) has values of -0.15 and -0.12 for the two catalyst films, respectively. For more negative potentials the rate approaches a plateau. The ρ value is up to 5 for catalyst C2 and up to 3 for catalyst C1.

For positive potentials the rate exhibits electrophobic behaviour; i.e. $\Delta r / \Delta V_{\text{WR}} > 0$ with ρ values up to 2.5 for catalyst C2 and up to 1.3 for catalyst C1. Equation [4] is also satisfied for positive potentials in the case of catalyst C2 with an α value of 0.15. This region is very narrow in the case of catalyst C1, where the rate quickly approaches a plateau with increasing potential. The reason for these, relatively minor, differences in the effect of potential on the catalytic rate for the two catalyst films, is not obvious but must be related to the different surface areas, thus different dispersions of the two catalyst films.

It is worth noting that similar differences are observed on the effect of V_{WR} on the current (Figs. 6a and 6b for the two catalyst films C1 and C2, respectively). These plots conform to the well-known Tafel equation (11, 12):

$$\ln(I/I_{0,a}) = \alpha_a F \Delta V_{\text{WR}} / RT, \quad I > 0, \quad [5]$$

$$\ln(I/I_{0,c}) = -\alpha_c F \Delta V_{\text{WR}} / RT, \quad I < 0, \quad [6]$$

where $I_{0,a}$, $I_{0,c}$ are the exchange currents for anodic and cathodic operation, which do not coincide in the present case, and α_a , α_c are the anodic and cathodic transfer coefficients, respectively. Although qualitatively the behaviour is similar for both catalysts, it is worth noting that the value of α_a

is high, i.e. 1.5 and 0.71 for catalysts C2 and C1, respectively, while α_c is lower, i.e. 0.38 for C2 and 0.23 for C1. As a result of these values both the rate and the current dependence on potential are more pronounced for catalyst C2 versus catalyst C1.

Figure 6b also shows the current-potential (Tafel) behaviour of the Au film of catalyst C2 before deposition of the dispersed Pt catalyst. The addition of Pt causes relatively small changes in the current-potential characteristics. The absolute value of the current increases with positive potentials and decreases with negative ones. These observations may reflect the stronger binding of oxygen on Pt versus Au. The main conclusion, however, of this comparison is that, apparently, only a relatively minor fraction of the three-phase boundaries Au-YSZ gas is occupied by the Pt crystallites.

Effect of Potential on the Kinetics

Figures 7 and 8 show the effect of catalyst potential on the kinetics of the catalytic reaction with respect to oxygen and ethylene, respectively. The rate exhibits maxima with respect both to oxygen and ethylene, indicating competitive adsorption and Langmuir-Hinshelwood-type kinetics. These figures show that electrophilic behaviour dominates ($\Delta r / \Delta V_{\text{WR}} < 0$) at high oxygen to ethylene ratios where the effect of potential is more pronounced. Figure 9a shows Arrhenius plots obtained at open-circuit and at various imposed catalyst potentials. The corresponding activation energies are plotted in Fig. 9b as a function of potential. As

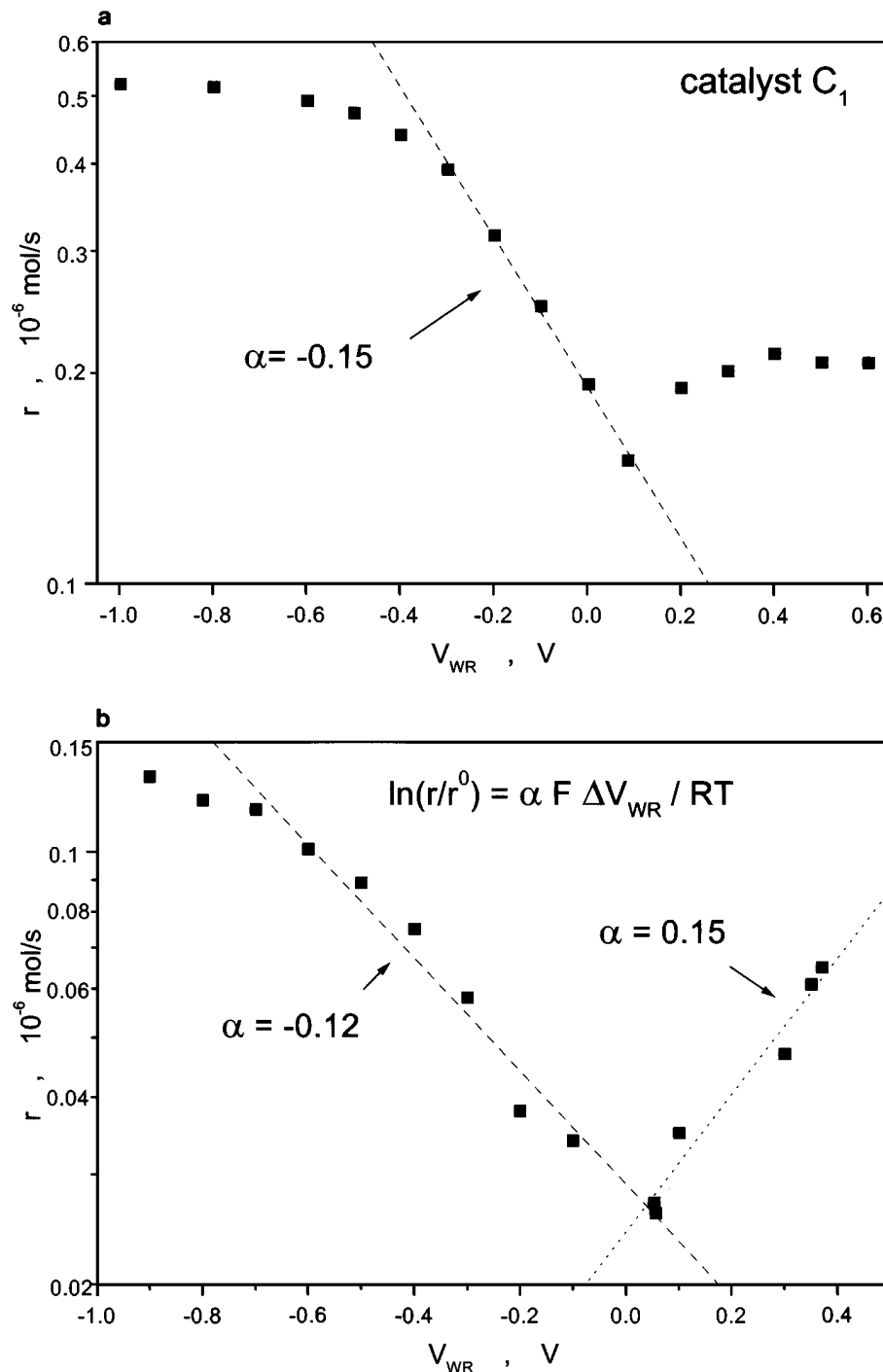


FIG. 5. Effect of the catalyst potential on the rate r for (a) catalyst C1 and (b) catalyst C2. Conditions: $T = 425^\circ\text{C}$, $P_{\text{O}_2} = 15 \text{ kPa}$, $P_{\text{C}_2\text{H}_4} = 0.1 \text{ kPa}$, flow = 400 ml/min, (a), and 621 ml/min (b), open-circuit rate: $r^0 = 0.15 \times 10^{-6} \text{ mol/s}$ (a) and $r^0 = 0.026 \times 10^{-6} \text{ mol/s}$ (b).

in several previous NEMCA studies (11, 12) the activation energy varies linearly with potential. In the present case it decreases with a slope of -0.5 . Figure 10 shows the effect of current on the magnitude of the rate time constant, τ , during galvanostatic transients. The latter is defined as the time required for the rate increase (or decrease) to reach 63% of its steady state value. As shown in the figure the measured

τ values are in very good qualitative agreement with

$$\tau \approx 2FN/I, \quad [7]$$

where N is Pt surface area ($0.38 \times 10^{-8} \text{ mol}$) measured via surface titration. This is valid both for positive applied currents (Fig. 10a) as well as for negative ones (Fig. 10b).

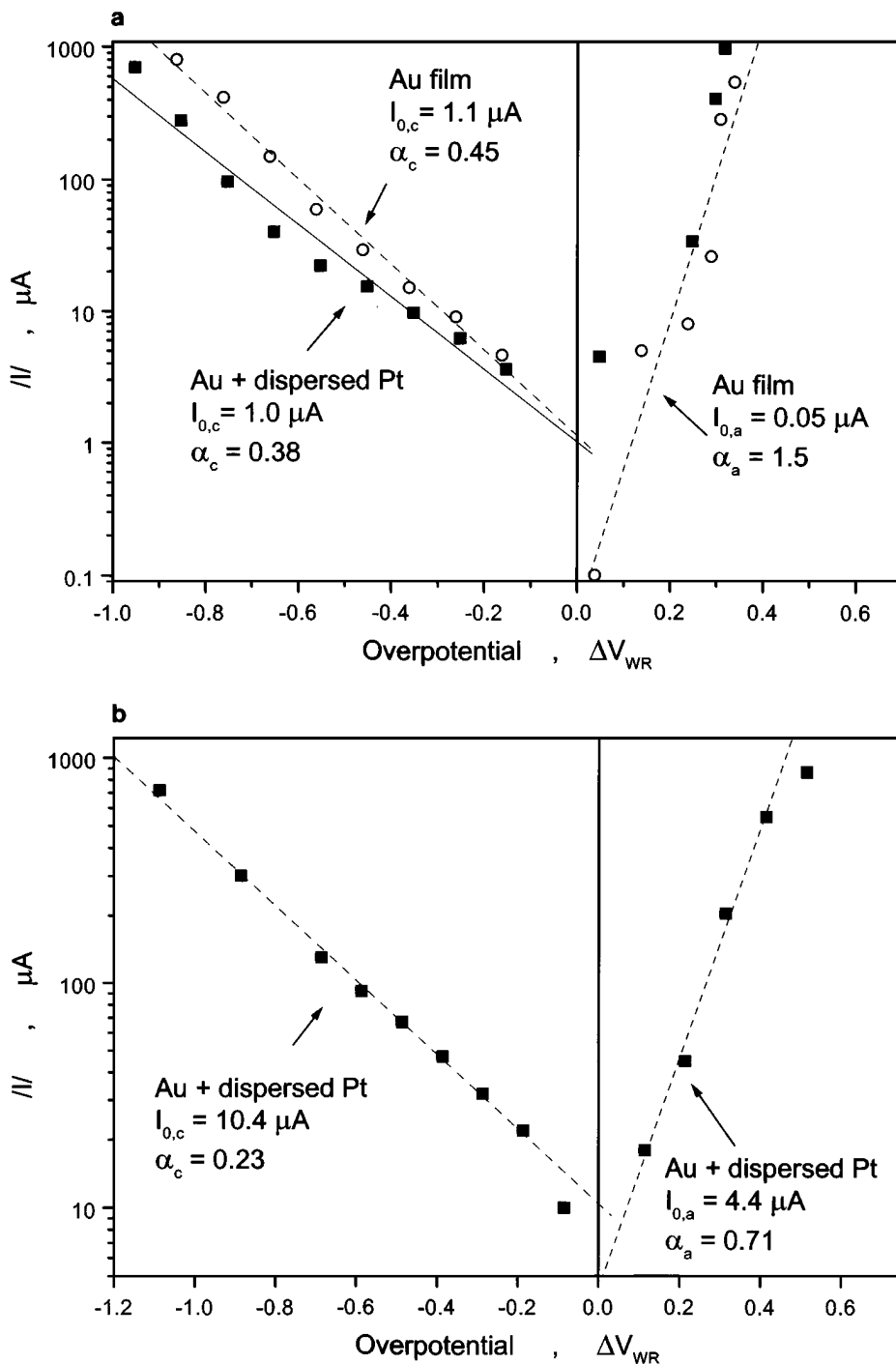


FIG. 6. Dependence of anodic ($I > 0$) and cathodic ($I < 0$) current on the catalyst overpotential for the gold working electrode before (open circles) and after (solid squares) the Pt impregnation for (a) catalyst C1 and (b) catalyst C2. Conditions: see Fig. 5.

In the latter case a better agreement with experiment can be obtained by the expression

$$\tau \approx 2FN\theta_O/I, \quad [8]$$

where θ_O is the coverage of oxygen on the Pt surface, e.g. Fig. 10b, where an assumed θ_O value of 0.25 provides a better fit to the data.

Since $2FN/I$ is the time required to form or remove a monolayer of oxygen on a surface with N sites, when it is supplied or removed at a rate $I/2F$ and the surface diffusion is fast, this observation provides strong support to the idea that the observed promotional phenomena are due to the electrochemically controlled migration of O^{2-} (at a rate $I/2F$) to or from the Pt catalyst surface. It is worth noting

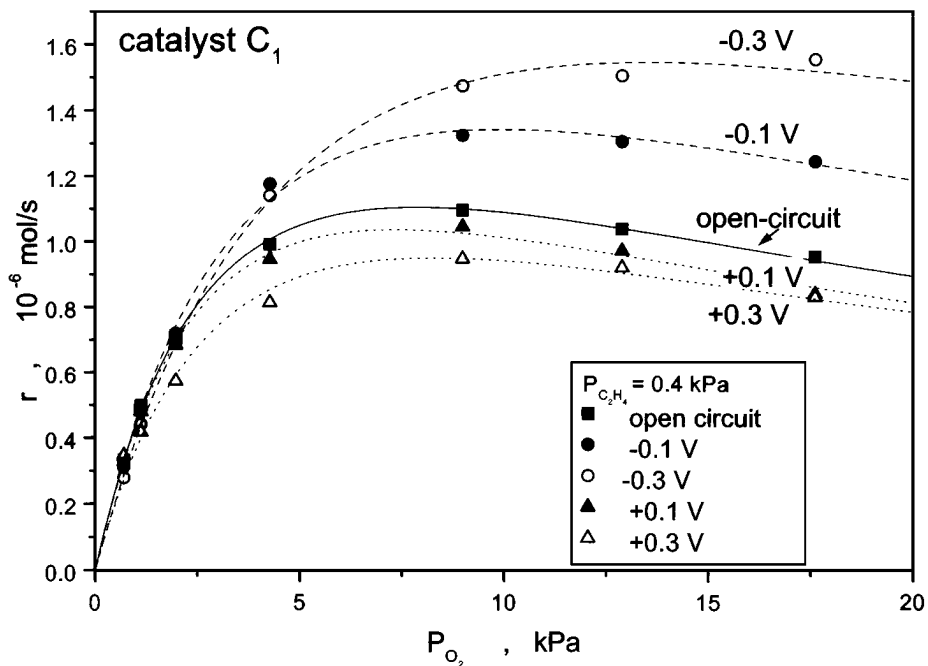


FIG. 7. Effect of the partial pressure of O_2 (P_{O_2}) on the rate r for open-circuit (squares) and $V_{WR} = -0.3$ V (open circles), -0.1 V (solid circles), $+0.1$ V (solid triangles), and $+0.3$ V (open triangles). Conditions: catalyst C1, $T = 426^\circ\text{C}$, $P_{C_2H_4} = 0.4$ kPa, flowrate = 480 ml/min.

that, since the coverage of oxygen on Au is generally very low, the Au surface serves only as a means of oxygen ion transport and thus does not contribute to any significant extent to the above relaxation time constants (Eqs. [7] and [8]).

DISCUSSION

The present results show that the effect of electrochemical promotion (NEMCA) can be induced on finely dispersed metal catalysts supported on a second, catalytically

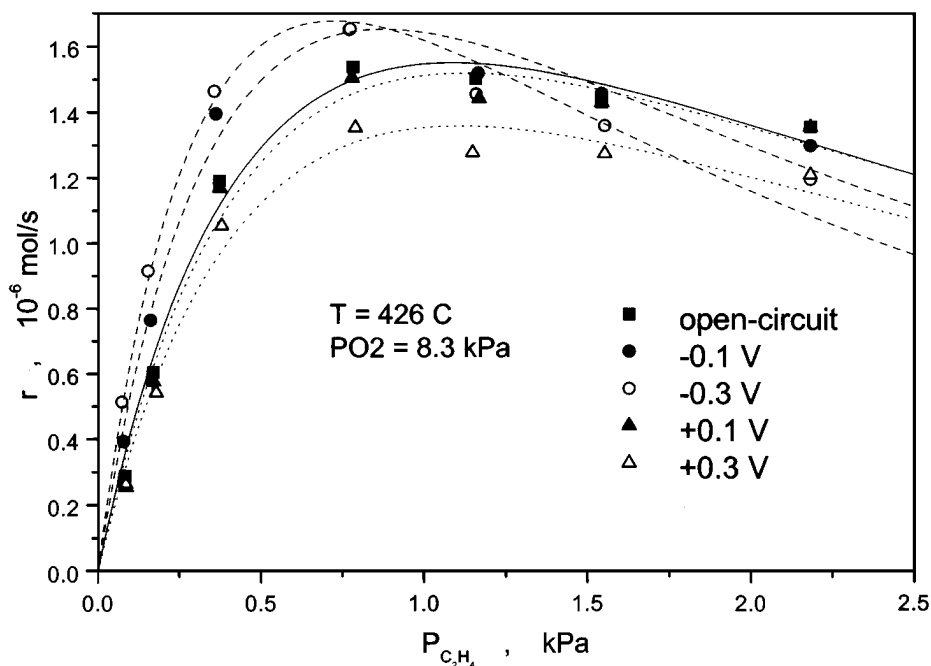


FIG. 8. Effect of the partial pressure of C_2H_4 ($P_{C_2H_4}$) on the rate r for open-circuit (squares) and $V_{WR} = -0.3$ V (open circles), -0.1 V (solid circles), $+0.1$ V (solid triangles), and $+0.3$ V (open triangles). Conditions: catalyst C1, $T = 426^\circ\text{C}$, $P_{O_2} = 8.3$ kPa, flowrate = 504 ml/min.

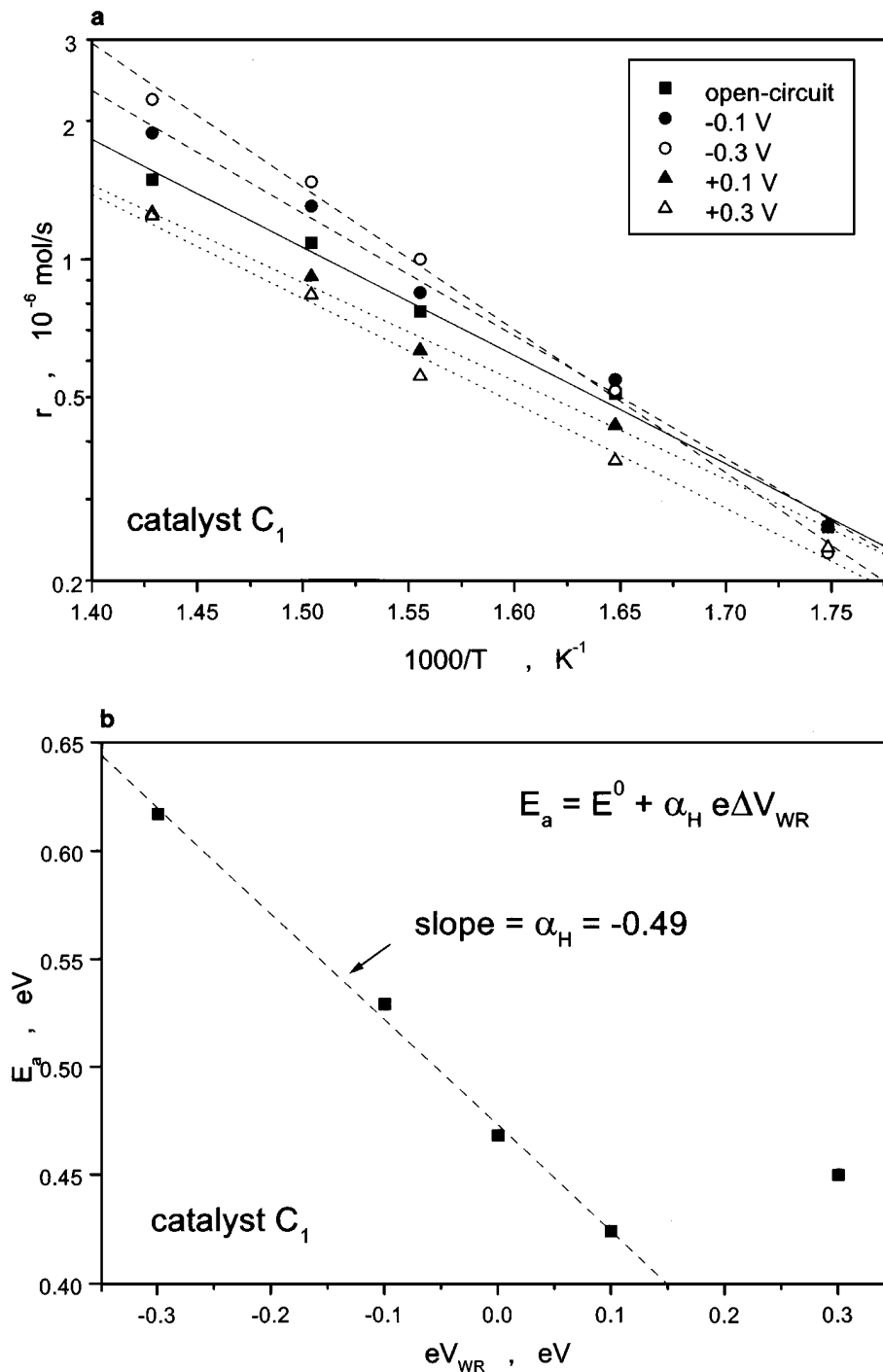


FIG. 9. (a) Arrhenius plots of the rate r for open-circuit (squares) and $V_{WR} = -0.3$ V (open circles), -0.1 V (solid circles), $+0.1$ V (solid triangles), and $+0.3$ V (open triangles); (b) effect of the catalyst potential V_{WR} on the apparent activation energy E_a . Conditions: catalyst C_1 , $P_{O_2} = 18.0$ kPa, $P_{C_2H_4} = 0.6$ kPa, flowrate = 400–500 ml/min.

inert metal. Consequently direct contact between the catalyst and the solid electrolyte is not necessary in order to induce electrochemical promotion. Furthermore, it is not necessary for the catalyst to be continuous. These results may be significant for the practical utilization of electrochemical promotion.

Two items need to be discussed: First the state of the Pt catalyst on the porous Au film and second the main features of the observed electrochemical promotional behaviour of ethylene oxidation.

Platinum-gold alloy catalysts prepared at temperatures above 500°C , have been studied for years primarily to

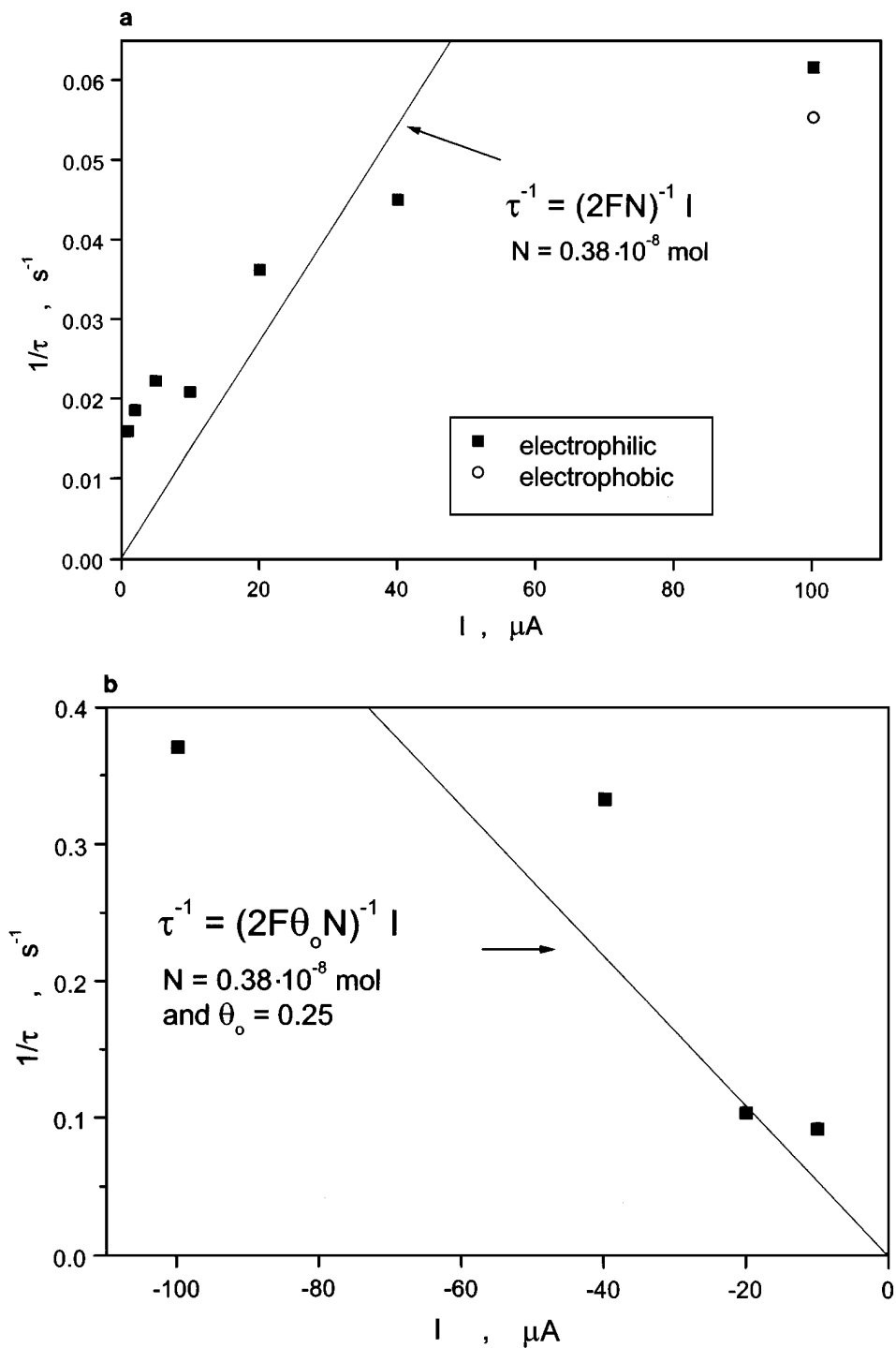


FIG. 10. Effect of the current I on τ^{-1} , where τ is the time constant measured during a galvanostatic transient experiment with I as the applied current; τ is obtained by fitting either $r/r^0 = \exp(-t/\tau)$ or $1 - \exp(-t/\tau)$ to the experimental data depending on the sign of the current and whether the reaction is electrophilic or electrophobic. (a) Positive values of I for electrophilic (squares, $T = 371^\circ\text{C}$, $P_{\text{O}_2} = 18.0 \text{ kPa}$, $P_{\text{C}_2\text{H}_4} = 0.6 \text{ kPa}$) and electrophobic behavior (circle, $T = 421^\circ\text{C}$, $P_{\text{O}_2} = 14.8 \text{ kPa}$, $P_{\text{C}_2\text{H}_4} = 0.1 \text{ kPa}$); (b) negative currents, electrophilic behavior ($T = 421^\circ\text{C}$, $P_{\text{O}_2} = 14.8 \text{ kPa}$, $P_{\text{C}_2\text{H}_4} = 0.1 \text{ kPa}$). Catalyst C2.

investigate ensemble effects during hydrogenation and skeletal transformation of hydrocarbons (21, 29–32) and during aqueous phase oxidation of alcohols (33).

The following factors show that the Pt catalyst was present in the form of small (<5nm) particles on the surface of the porous Au electrode:

1. Pt-Au alloying is known to occur above 450°C (21, 25, 29–33). Below this temperature no alloying takes place. The maximum temperature of the present kinetic investigation was 421°C.

2. The catalytic activity of the Pt/Au catalyst remained constant throughout the entire kinetic investigation, i.e. over a period of several weeks. Consequently there is no sign of any Pt loss due to alloying throughout the investigation.

3. The measured Pt surface area ($N=0.38 \times 10^{-8}$ mol Pt) corresponds to a Pt surface area of 1.5 cm² which is well below the estimated surface area of the Au film, i.e., 100 to 300 cm² which is typical of noble metal films deposited with Engelhard pastes (11, 12). Consequently the total mass of Pt is insignificant in relation to the mass of the Au film and is not sufficient to form a monolayer.

4. The measured turnover frequencies are of the same order of magnitude as those measured on Pt/YSZ films (34) and on well-dispersed Pt/YSZ catalysts (36) (Table 1).

5. The catalytic rate time constants, τ , during current application (Figs. 3 and 4) are in very good agreement with the parameter $2FN/I$ (Fig. 10) which is the time required to form a monolayer of oxygen on the Pt surface. Consequently the catalyst can be perceived as small Pt crystallites (dispersion 0.2 to 1) supported on the Au electrode.

The main features of the observed electrochemical promotion are in good qualitative agreement with previous NEMCA studies with film catalyst electrodes. Thus the order of magnitude of $|\Delta|$ conforms to

$$|\Delta| \approx 2Fr^0/I_0 \quad [9]$$

TABLE 1
Comparison of Turnover Frequencies

Literature	Catalyst C ₁ ($N=1.8 \times 10^{-8}$ mol)
Reference (34) Catalyst: Pt film on YSZ T = 425°C, 6.4% O ₂ , 0.4% C ₂ H ₄ TOF = 18 s⁻¹	T = 425°C, 4.3% O ₂ , 0.4% C ₂ H ₄ TOF = 55 s⁻¹
Reference (36) Catalyst: 0.5% Pt dispersed on YSZ T = 250°C, 6% O ₂ , 1% C ₂ H ₄ TOF = 2.1 s⁻¹	T = 250°C, 8.3% O ₂ , 1.1% C ₂ H ₄ ^bTOF = 5.8 s⁻¹
T = 425°C, 6% O ₂ , 1% C ₂ H ₄ ^aTOF = 490 s⁻¹	T = 250°C, 8.3% O ₂ , 1.1% C ₂ H ₄ TOF = 83 s⁻¹

^a Calculated using $E_a = 94$ kJ/mol (Ref. (36)).

^b Calculated using $E_a = 46$ kJ/mol.

and also, as previously noted, the magnitude of τ conforms to

$$\tau \approx 2FN/I. \quad [7]$$

Previous electrochemical promotion studies of ethylene oxidation on Pt/YSZ (34, 35) have shown a pronounced electrophobic rate enhancement with positive potentials under conditions where the rate is first order in ethylene and zero order in oxygen, indicating weak adsorption of ethylene (34) and electrophilic behaviour with negative potentials under conditions of competitive chemisorption of oxygen and ethylene (35). In the present investigation, where the kinetics (Figs. 7 and 8) suggest competitive adsorption of ethylene and oxygen, electrochemical promotion causes a small electrophobic enhancement for positive potentials at high oxygen to ethylene ratios, while lower oxygen to ethylene ratios lead to electrophilic behaviour, even at positive potentials. Electrophilic behaviour dominates at negative potentials with ρ values up to five.

The electrophobic behaviour at high oxygen to ethylene ratios and high catalyst potentials (Figs. 5a and 5b) can be explained, as previously (11, 12), by taking into account the effect of increasing catalyst potential and work function on the chemisorptive bond strength of oxygen; TPD analysis (16) and rigorous quantum mechanical calculations (18) have shown that the binding energy of oxygen on Pt decreases linearly with increasing work function. The effect is primarily due to the repulsive lateral interactions between the electrochemically supplied ionic oxygen and the more neutral and more reactive normally chemisorbed atomic oxygen. Thus under conditions where the Pt surface is almost entirely oxygen-covered, an additional supply of O²⁻ weakens the Pt = O chemisorptive bond, the cleavage of which is rate limiting and thus accelerates the catalytic rate of oxidation.

Decreasing the catalyst potential below its open-circuit also causes a pronounced enhancement in the rate (Figs. 5a and 5b). This electrophilic rate enhancement might at a first glance appear to be directly related to the removal of oxygen in the form of O²⁻ from the Pt catalyst to the YSZ solid electrolyte and the concomitant creation of free reaction sites. It should be emphasized, however, that the rate of removal of oxygen from the Pt surface, $I/2F$, is typically of the order of 10⁻⁹ mol O/s while the rate of the catalytic reaction and the, equal at steady state, rate of oxygen adsorption is much higher, typically of the order of 10⁻⁷ mol/s (Figs. 3, 5). Consequently the observed pronounced rate enhancement (Figs. 3, 5) cannot be attributed to such a simple mechanism alone. The explanation can be sought in the fact that the imposed decrease in catalyst potential and concomitant decrease in catalyst work function (2, 11, 12) can be realized at the molecular level by a significant decrease in the coverage of oxygen, which is an electron acceptor and thus tends to increase the catalyst work function, and by a concomitant increase in the coverage of adsorbed ethylene which is an

electron donor and thus tends to decrease the catalyst work function (11, 12). This increase in ethylene versus oxygen coverage at negative potentials is also manifest indirectly by the kinetics (Fig. 8), where for negative potentials the rate is enhanced significantly at low $P_{C_2H_4}$ values and where for high $P_{C_2H_4}$ values the rate becomes of negative order in ethylene in a much more pronounced manner than in the cases of positive potentials or open-circuit operation.

It is interesting to note the striking similarity of the NEMCA behaviour of the present C_2H_4 oxidation system with that of the CO oxidation system on Pt/YSZ films (37), i.e. electrophilic behaviour with negative potentials with ρ values up to 5, weak electrophobic behaviour with positive potentials (37). In a recent paper Harkness *et al.* (38) have used isotopic labeling to show that ethylene oxidation on dispersed Pt proceeds via intermediate formation of CO. It is therefore likely that reactive ethylene chemisorption producing chemisorbed CO proceeds fast on the present dispersed Pt/Au catalyst and that the rate limiting step of the overall reaction is the reaction between coadsorbed CO and O. This can explain the comparable propensity of the two species for adsorption as manifest by the rate maxima with respect to both C_2H_4 and O_2 (Figs. 7 and 8), as well as the fact that electrochemical promotion does not cause any pronounced shift in the location of these maxima. Since CO behaves primarily (11, 12) as an electron acceptor, similar to oxygen (11, 12), varying potential and work function are expected to have only a small effect in the relative propensity of the two species for chemisorption on the Pt surface. This can also explain the observed increase in apparent activation energy with decreasing catalyst potential and work function (Fig. 9). Decreasing potential strengthens the chemisorptive bond of both CO and O, thus increasing the apparent activation energy.

In summary all the observed features of electrochemical promotion for the present dispersed Pt on Au catalyst are similar to previous electrochemical promotion studies on metal film catalysts. They can thus be rationalized by the same considerations invoked to explain electrochemical promotion on metal catalyst films (11, 12, 39), i.e. by considering the effect of varying catalyst potential and work function on the chemisorptive binding strength of electron acceptor and donor adsorbates. The ability to induce electrochemical promotion on finely dispersed metal catalysts may be of considerable practical importance.

ACKNOWLEDGMENTS

We thank EPRI and the EPET-II and PENED programmes of the Hellenic Secretariat of Research and Technology for financial support and our reviewers for some useful suggestions.

REFERENCES

- Vayenas, C. G., Bebelis, S., and Neophytides, S., *J. Phys. Chem.* **92**, 5083 (1988).
- Vayenas, C. G., Bebelis, S., and Ladas, S., *Nature* **343**, 625 (1990).
- Politova, T. I., Sobyenin, V. A., and Belyaev, V. D., *React. Kinet. Catal. Lett.* **41**, 321 (1990).
- Basini, L., Cavalca, C. A., and Haller, G. L., *J. Phys. Chem.* **88**, 10853 (1994).
- Harkness, I., and Lambert, R. M., *J. Catal.* **152**, 211 (1995).
- Varkaraki, E., Nicole, J., Plattner, E., Comninellis, Ch., and Vayenas, C. G., *J. Appl. Electrochem.* **25**, 978 (1995).
- Tsiplakides, D., Neophytides, S., Enea, O., Jaksic, M. M., and Vayenas, C. G., *J. Electrochem. Soc.* **144**(6), 272 (1997).
- Makri, M., Buekenhoudt, A., Luyten, J., and Vayenas, C. G., *Ionics* **2**, 282 (1996).
- Pliangos, C., Yentekakis, I. V., Ladas, S., and Vayenas, C. G., *J. Catal.* **159**, 189 (1996).
- Petrolekas, P., Balomenou, S., and Vayenas, C. G., *J. Electrochem. Soc.* **145**(4), 1202 (1998).
- Vayenas, C. G., Jaksic, M. M., Bebelis, S., and Neophytides, S., in "Modern Aspects of Electrochemistry" (J. O'M. Bockris, B. E. Conway, and R. E. White, Eds.), Vol. 29, Plenum, New York, 1996.
- Vayenas, C. G., and Yentekakis, I. V., Electrochemical modification of catalytic activity, in "Handbook of Catalysis" (G. Ertl, H. Knotzinger, and J. Weitcamp, Eds.), p. 1310. VCH Publishers, Weinheim, 1997.
- Vayenas, C. G., Ioannides, A., and Bebelis, S., *J. Catal.* **129**, 67 (1991).
- Ladas, S., Kennou, S., Bebelis, S., and Vayenas, C. G., *J. Phys. Chem.* **97**, 8845 (1993).
- Palermo, A., Tikhov, M. S., Filkin, N. C., Lambert, R. M., Yentekakis, I. V., and Vayenas, C. G., *Stud. Surf. Sci. Catal.* **101**, 513 (1996).
- Neophytides, S., and Vayenas, C. G., *J. Phys. Chem.* **99**, 17063 (1995).
- Makri, M., Vayenas, C. G., Bebelis, S., Besocke, K. H., and Cavalca, C., *Surf. Sci.* **369**, 351 (1996).
- Pacchioni, G., Illas, F., Neophytides, S., and Vayenas, C. G., *J. Phys. Chem.* **100**, 16653 (1996).
- Boudart, M., and Djega-Marriadassou, G., "Kinetics of Heterogeneous Catalytic Reactions," Princeton Univ., Princeton, NJ, 1984.
- Neophytides, S. G., Tsiplakides, D., Stonehart, P., Jaksic, M. M., and Vayenas, C. G., *Nature* **370**, 45 (1994).
- Ponec, V., and Bond, G. C., in "Catalysis by Metals and Alloys," Studies in Surface Science and Catalysis (B. Delmon and J. T. Yates, Eds.), p. 61. Elsevier, Amsterdam, 1995.
- Stoukides, M., and Vayenas, C. G., *J. Catal.* **64**, 18 (1980).
- Yentekakis, I. V., and Bebelis, S., *J. Catal.* **137**, 278 (1992).
- Karavasili, Ch., Bebelis, S., and Vayenas, C. G., *J. Catal.* **160**, 205 (1996).
- Hözl, J., and Schulte, F. K., in "Solid Surface Physics" (R. B. Anderson and E. Niekisch, Eds.), p. 1. Springer-Verlag, Berlin, 1979.
- Chang, S. C., Jiang, X., Roth, J. D., and Weaver, M. J., *J. Phys. Chem.* **95**, 5378 (1991).
- Nicole, J., Tsiplakides, D., Wodiunig, S., and Comninellis, Ch., *J. Electrochem. Soc.* **144**(2), L312-L314 (1997).
- Zipprich, W., Wiemhöfer, H.-D., Vohrer, U., and Göpel, W., *Ber. Bunsenges. Phys. Chem.* **99**, 1406 (1995).
- Cinneide, O. A., and Gault, F. G., *J. Catal.* **37**, 311 (1975).
- Clarke, J. K. A., Manninger, I., and Baird, T., *J. Catal.* **54**, 230 (1978).
- Sachtler, J. W. A., and Somorjai, G. A., *J. Catal.* **81**, 77 (1983); **89**, 35 (1984).
- Salmeron, M., Ferrer, S., Jazsar, M., and Somorjai, G. A., *Phys. Rev. B* **28**, 1158 (1983).
- Mallat, T., Bodnar, Z., Baiker, A., Greis, O., Ströbig, H., and Reller, A., *J. Catal.* **142**, 237 (1993).
- Bebelis, S., and Vayenas, C. G., *J. Catal.* **118**, 125 (1989).
- Marwood, M., and Vayenas, C. G., *J. Catal.* **168**, 538 (1997).
- Pliangos, C., Ph.D. thesis, University of Patras, 1995.
- Yentekakis, I. V., and Vayenas, C. G., *J. Catal.* **111**, 170 (1988).
- Harkness, I. R., Hardacre, C., Lambert, R. M., Yentekakis, I. V., and Vayenas, C. G., *J. Catal.* **160**, 19 (1996).
- Bebelis, S., and Vayenas, C. G., *J. Catal.* **138**, 570 (1992).